Unclassified

SECURITY CLASSIFICATION OF THIS PAGE (When Data Entered)

REPORT DOCUMENTATION PAGE		READ INSTRUCTIONS BEFORE COMPLETING FORM
1. REPORT NUMBER	2. GOVT ACCESSION NO.	3. RECIPIENT'S CATALOG NUMBER
4. TITLE (and Subtitle) Epitaxial Growth of Single Crystal Films		5. TYPE OF REPORT & PERIOD COVERED Final Report 10/04/75 - 05/31/80
		6. PERFORMING ORG. REPORT NUMBER ERC41001.30FR
7. AUTHOR(s) M. D. Lind		8. CONTRACT OR GRANT NUMBER(s) NAS8-31733
9. PERFORMING ORGANIZATION NAME AND ADDRESS Electronics Research Center Rockwell International Corporation 1049 Camino Dos Rios, Thousand Oaks, CA 91360		10. PROGRAM ELEMENT, PROJECT, TASK AREA & WORK UNIT NUMBERS
11. CONTROLLING OFFICE NAME AND ADDRESS National Aeronautics & Space Administration Marshall Space Flight Center, AL 35812		12. REPORT DATE May 31, 1980 13. NUMBER OF PAGES 35
14. MONITORING AGENCY NAME & ADDRESS (if different from Controlling Office)		15. SECURITY CLASS. (of this report) Unclassified 15a. DECLASSIFICATION/DOWNGRADING SCHEDULE

16. DISTRIBUTION STATEMENT (of this Report)

(NASA-CR-161544) EPITAXIAL GROWTH OF SINGLE CRYSTAL FILMS Final Report, 4 Oct. 1975 - 31 May 1980 (Rockwell International Corp., Thousand Oaks) 36 p HC A03/MF A01 CSCL 20L

N80-31242

Unclas
G3/76 28480

17. DISTRIBUTION STATEMENT (of the abstract entered in Block 20, if different from Report)

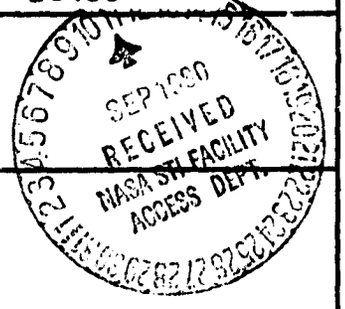

18. SUPPLEMENTARY NOTES

19. KEY WORDS (Continue on reverse side if necessary and identify by block number)

liquid phase epitaxy, gallium arsenide, sounding rocket, SPAR program.

20. ABSTRACT (Continue on reverse side if necessary and identify by block number)

An experiment in gallium arsenide liquid phase epitaxy was performed successfully on the SPAR VI flight October 17, 1979. The design, fabrication, and testing of the experimental apparatus, and the performance and results of the experiment are discussed.

DD FORM 1 JAN 73 1473 EDITION OF 1 NOV 65 IS OBSOLETE

Unclassified

SECURITY CLASSIFICATION OF THIS PAGE (When Data Entered)

1.0 INTRODUCTION

A. Natural Convection in Crystal Growth Processes

In nearly all crystal growth processes, fluid density variations caused by variations in temperature or composition can result in fluid motion called natural convection. This can be a significant and even predominant factor in the transfer of material and heat in these processes. These flows can have adverse effects on growth rates, liquid-solid interface shapes, and distributions of impurities or dopants. In some cases, this is believed to contribute to the formation of excessive structural defects or compositional inhomogeneities in the crystals produced. These imperfections are likely to impair the performance of devices made from such materials, and can be a particularly acute problem in the production of large quantities of devices.

Natural convection occurs in a fluid when its Rayleigh or Grashof number exceeds a critical value. In the discussion which follows, we shall consider three cases: (1) For a vertical temperature difference, ΔT_V, across a fluid depth, d, the Rayleigh number

$$N_{Ra} = g \alpha \Delta T_V d^3/\kappa\nu \qquad (1)$$

is appropriate. Here g is the gravitational acceleration, α is the volume thermal expansion coefficient, κ is the thermal diffusivity, and ν is the kinematic viscosity of the fluid; (2) The equivalent Rayleigh number for a vertical solute concentration gradient, ΔC_V, is

$$N_{Ra} = g \beta \Delta C_V d^3/D\nu \qquad (2)$$

where β is the change in volume per unit change in solute concentration and D is the diffusion coefficient of the solute; (3) For a horizontal temperature difference, ΔT_H, across a fluid length, ℓ, the Grashof number

$$N_{Gr} = g \alpha \Delta T_H \ell^3/\nu^2 \qquad (3)$$

is appropriate. The critical values of the Rayleigh and Grashof numbers for natural convection in a particular crystal growth process depend on several factors, and can vary by an order of magnitude from one process to another. For the present discussion, it is not necessary to specify the critical values for any particular process, but only to note from the forms of the above three equations that to suppress natural convection in any given fluid, the Rayleigh or Grashof number can be reduced by reducing ΔT, ΔC, d, ℓ, or g. (In some special cases, natural convection can be suppressed by adding a substance to the fluid which increases its viscosity, ν, but this does not apply to the fluids to be discussed here).

Through the development of space flight in recent years, the investigation of crystal growth with reduced g has become possible. Several crystal growth experiments were performed during the Apollo, Skylab, and Apollo-Soyuz flights. During the interval between the Apollo-Soyuz flight (1975) and the first Space Transportation System flights (early '80's) the National Aeronautics and Space Administration is conducting a Space Processing Applications Rocket (SPAR) Project. This project utilizes Black Brant VC sounding rockets, which can carry payloads of several hundred pounds and provide durations of weightlessness of about five minutes.

B. Liquid Phase Epitaxy (LPE) of Gallium Arsenide

Gallium arsenide LPE appeared to be an appropriate process for investigation on a SPAR flight for the following reasons: (1) the process variables, including growth temperatures and rates, are compatible with the capabilities of the Black Brant VC flights; and (2) the numerous important technological applications of gallium arsenide LPE films have stimulated broad interest in this process and material, and therefore there was available

ample background information on which to base the design of a space flight experiment, and with which to compare results.

In most gallium arsenide LPE processes in normal gravity, the substrate is horizontal and a well of molten supersaturated solution of arsenic in excess gallium is slid horizontally over the substrate to cover it for a time long enough to grow the desired epitaxial film thickness, after which growth is terminated by sliding the solution away from the substrate (see Figure 1).

In solutions of arsenic in gallium, the diffusion coefficient, D, is much smaller than the thermal diffusivity, κ, and, therefore, solute concentration gradients predominate over temperature gradients in causing natural convection (see Equations 1 and 2, above). To suppress convection due to solute concentration gradients, it is necessary to limit the depth of solution, d, to 1-2 mm. Care must also be taken to minimize horizontal temperature gradients (ΔT_H in Equation 3) in order to suppress the convection that they would cause.

Until now, these ways of suppressing convection appear to have sufficed, and LPE processes routinely yield gallium arsenide and other compound semiconductor films adequate in quality for their applications. Therefore, the principal objective of the SPAR experiment was to improve our understanding of the process, and in particular, to confirm theoretical analyses of material transport and growth kinetics, rather than to achieve improved film quality. However, it is probable that natural convection is often not completely eliminated in conventional LPE processes in normal gravity, and that eventually the residual effects may be found to limit the usefulness of the films.

Furthermore, if future applications require larger wafer dimensions, the approach of reducing g may be the only one which can succeed. Thus, LPE processes in near-zero gravity may eventually turn out to be useful for producing superior films of gallium arsenide and other compound semiconductors.

For the process investigated, the epitaxial film thickness for the case of material transport by diffusion only is given by[1]

$$d_f = \frac{2\Delta T}{C_s m} \left(\frac{Dt}{\pi}\right)^{\frac{1}{2}} \qquad (4)$$

where ΔT = supercooling interval

C_s = concentration of arsenic in crystalline gallium arsenide

m = slope of the liquidus line[2]

$D = 5000e^{-20000/T}$, diffusion coefficient of arsenic in liquid gallium[3]

t = growth time

Evaluation of (4) with a growth temperature $T = 990°K$, $\Delta T = 10°K$, and growth time $t = 60$ sec., all of which can be achieved on the Black Brant VC flights, results in $d_f \sim 1\mu m$. This is a desirable thickness for some gallium arsenide devices, such as field effect transistors.

II. Apparatus and Procedure for SPAR Experiment

A. Description of Apparatus

A self-contained LPE processor suitable for the Black Brant VC payload was designed and fabricated (see Figures 2-9). It is mounted in two adjacent rocket sections, 21.6 and 18.1 cm in length. The outside diameter of these sections is that of the rocket, 43.8 cm. The processor is composed of four major subsystems:

1. Furnace

The LPE processor has a specially designed tubular resistance heated furnace mounted in the upper rocket section (Fig. 6). Two doors in the section provide access for loading the furnace. The heating element is nichrome wire wound helically on a ceramic tube 2.5 cm in inside diameter and 9.5 cm long. The windings are spaced closer at each end to minimize axial temperature gradients. The insulation between the inner and outer tubes of the furnace is an asbestos based blanket. All other parts of the furnace are stainless steel. Its outermost shell is 10.2 cm in diameter and approximately 28 cm long. The maximum temperature of the furnace is approximately 1300°K.

2. Atmospheric Control

Provision is made for a flowing hydrogen atmosphere inside the furnace (see Figure 9). This system includes the following components: (1) a 300 cm^3, 2000 psi supply cylinder, (2) pressure regulator, (3) flow-rate valve, (4) bubbler to prevent gas back-streaming, (5) non-propulsive exhaust, (6) two quick-release umbilical connectors used as inlet and exhaust during ground operation, and for loading the hydrogen supply, and (7) a solenoid valve for routing the exhaust through the umbilical connector during ground operation, and through the non-propulsive vents during the flight.

All components are stainless steel. The bubbler uses a magnetic fluid of very low vapor pressure held in place by a permanent magnet. The system is designed to operate at pressures up to 30 psig and flow rates up to a few hundred cm^3 per minute.

3. Slider

The slider is operated pneumatically with retraction by a spring when the gas pressure is released. It is enclosed in a cartridge (see Figure 7) which is removable through a door in the side of the rocket section to facilitate loading. A 50 cm^3 cylinder pressurized to 100 psig supplies gas for operating the slider. A solenoid valve applies the pressure and releases it, and a microswitch indicates the slider position. The slider accommodates two 1.1 x 1.3 cm substrates located on opposite sides of the solution cavity in an assembly fabricated from graphite (Figure 8). The depth of the solution cavity, 6.35 mm, was intentionally made great enough to result in natural convection in normal gravity. A spring-loaded volume compensator allows for expansion and contraction of the molten solution with temperature changes. Chromel-Alumel thermocouples in alumina sheaths are located in grooves on either side of the graphite assembly adjacent to the solution cavity.

4. Microprocessor

A microprocessor thermally isolated in the lower rocket section controls the entire process, including temperature control and operation of the two solenoid valves in the gas system. The

microprocessor was provided by the Marshall Space Flight Center and is identical to that used in their General Purpose Rocket Furnace (GPRF). To simplify the adaptation of the microprocessor to the LPE processor, the furnace heating element was made to match that of the heating elements in the GPRF, and the same type of thermocouple was used. The growth temperature set point, solenoid valve operation times, and power-off time are set by adjusting potentiometers. In addition to controlling the process, the microprocessor provides readouts of the temperatures sensed by the two thermocouples, the actual times of substrate insertion and retraction, and the hydrogen supply pressure. These data are telemetered to the ground control facility at the launchsite during the flight. For ground and pre-launch operations, the temperature of the furnace and the operation of the slider are controlled manually, and the temperatures, slider position, and hydrogen pressure are indicated at the control panel.

The electrical power is provided by a 34 volt D.C. power supply during ground and prelaunch operations, and by batteries in a service module in the sounding rocket during the flight.

Besides the electrical control panel, the ground support equipment includes a gas control panel with valves, flow-rate meter, bubbler, and an oil-less vacuum pump for manual ground and pre-launch operation of the hydrogen system. It was designed to be used for evacuating the hydrogen system to a pressure of a few microns and back-filling with hydrogen to start the process.

The flow-rate meter is used to adjust the internal flow-rate valve. The external bubbler was provided in order that the system could be operated without filling the internal one. To ensure against spillage the internal bubbler was not filled until the rocket was in position in the launch tower.

The entire processor and ground support equipment were designed to be as multi-purpose as possible. The slider cartridge can readily be modified for different materials, and can be replaced by other kinds of sample cartridges. Gases other than hydrogen can be used for atmospheric control. The temperature-time program can readily be changed for other materials. Furthermore, the processor can be adapted to Space Transportation System flights with or without different packaging.

B. Procedure

For each pre-flight test of the apparatus and for the flight itself, the planned growth temperature was 990°K. For each, the solution was first saturated at a temperature in the range of 10-15°K above the planned growth temperature. The saturation step was performed in the flight apparatus, equipped with the same graphite slides to be used in the growth step. The slider was loaded with a fresh charge of pure gallium and two freshly cleaned gallium arsenide source wafers. The furnace temperature was raised to the desired saturation temperature, and the slider was operated to bring the wafers into contact with the gallium. The solution was allowed to equilibrate for one hour before the source wafers were retracted. The entire saturation step was performed with manual control of the temperature and slider position.

Two freshly cleaned substrate wafers cut perpendicular to the 100 direction were loaded in the slider for the growth step. The temperature-time profile of the growth step, shown in Figure 10, indicates the procedure followed in this step. Ninety minutes before the launch, the solution temperature was raised to 1050°K, and then beginning at the launch was lowered at a rate that allowed the growth temperature, 990°K, to be reached within the first four minutes of the flight. By this time, the near-zero gravity condition was well established, and the fluid motions induced by the launch were damped out. Growth was started at this time and terminated after one minute, well before the end of the near-zero gravity portion of the flight. Up to the time of the launch, the temperature was controlled manually. At the time of the launch, control of the process was transferred to the microprocessor.

Throughout the pre-flight tests of the apparatus and during the saturation step before the flight, the thermocouple outputs were monitored with a potentiometer giving much higher precision than the microprocessor readouts. This was necessary for sufficiently precise control of the supercooling interval, ΔT.

A hydrogen pressure of 5 psig and flow-rate of 100 cm^3 per minute were used for all pre-flight tests and for the flight. To provide adequate hydrogen for the flight, the hydrogen reservoir was pressurized to 600 psig before the launch.

III. Pre-Flight Testing

The LPE processor and its ground support equipment were subjected to three phases of pre-flight testing. The first was a series of engineering development tests to ensure that the apparatus could perform all its intended functions reliably and safely. These included vibrational, acceleration, and pressurization tests and repetitive functional tests. As may be expected for apparatus of the complexity of the LPE processor, the tests revealed the need for some modifications. The major modifications were (1) addition of a stainless steel fixture to support the graphite parts of the slider, which were found to be too fragile to withstand the mechanical loads to which they were subjected, (2) better electrical isolation of the thermocouples from the graphite parts, which was a requirement of the microprocessor circuitry misunderstood at first, and (3) improved thermal isolation of the microprocessor to correct the problem of a small upward drift of the furnace temperature caused by heating of the microprocessor by the adjacent hot furnace. After these modifications, the apparatus performed satisfactorily throughout the remainder of the pre-flight tests and the flight.

In the second phase of pre-flight testing, several epitaxial films were grown in the apparatus by simulating the pre-launch and flight procedures as closely as possible. The purposes of these tests were (1) to determine suitable temperatures for the process, (2) to verify the correctness of the pre-set slider operation and power-off times, hydrogen pressures, and hydrogen flow-rate, (3) to perform necessary

calibrations, and (4) to obtain experimental control samples for comparison with the flight samples. The test results indicated the growth temperature, 990°K, solution saturation temperature, 1000°K, and the pre-set times, pressures, and flow-rate to be suitable. The best epitaxial films were obtained in the last two tests, and are described in Section IV with the results of the flight eperiment.

The hydrogen flow-rate meter was calibrated by determining the times required to collect one liter of hydrogen for various flow-rate meter readings. The calibration data are shown in Figure 11, which indicates the correct readings for the desired rate of 100 cm^3 per minute.

The rate of hydrogen consumption was measured by recording the pressure in the hydrogen reservoir at five-minute intervals until depletion. This was done for several different initial pressures, with a flow-rate of 100 cm^3 per minute in each case. At the end of each test, the flow-rate fell from 100 cm^3 per minute to zero within a five-minute interval. Figure 12 shows the hydrogen pressure as a function of time for an initial pressure of 600 psig. These data agree with a simple calculation of the expansion of 300 cm^3 of gas under a pressure change from 600 psig to atmospheric pressure.

The pre-flight tests indicated that with power off the furnace cools from the growth temperature to about 300°K in two hours. An initial hydrogen pressure of 600 psig was chosen to provide for continued flow for this period and virtually complete depletion of the hydrogen at the end of the period.

The approximate power consumption of the processor was determined during the pre-flight tests. With the power limited to 300 watts, the furnace reaches 1050°K in fifteen minutes. Maintenance of this temperature requires approximately 200 watts, and of the growth temperature, 990°K, approximately 170 watts.

The third phase of pre-flight testing consisted of various full and partial functional tests at Marshall Space Flight Center, Goddard Space Flight Center, and White Sands Missile Range before and during the integration of the payload and rocket. During this phase, the microprocessor was modified by Marshall Space Flight Center personnel to improve its stability with variations in temperature, and thereby further ensure stability in the furnace temperature control.

IV. Results and Conclusions

The flight experiment was performed successfully on the SPAR VI flight on October 17, 1979. The processor functioned well throughout the flight. Epitaxial films of about the thickness expected were produced. They are shown along with pre-flight test results in Figure 13. Although the films grown during the flight are less smooth than the best films produced during pre-flight tests, they appear to be a satisfactory result for an initial space-flight experiment.

When the slider was removed from the furnace after the flight, it was in good condition, with the slides fully retracted. Later, after the slider had been returned to our laboratory and opened to remove the wafers, the solution cavity remained completely filled, confirming that there had been no leakage of solution dur-

ing the flight. On retraction of the slides, the solution had been swept from the wafers satisfactorily and the amount of gallium remaining on them was small.

Strip chart recordings of data telemetered to the ground during the flight also indicate satisfactory performance of the experiment. The recorded times of slider insertion and retraction were T + 262 sec. and T + 338 sec., respectively, both of which are within specifications. The recorded H_2 supply pressure was 640 psi at T + 0, and decreased uniformly to 620 psi at T + 700 sec., which also is within specifications. The recorded furnace temperatures are approximately as expected, but are relatively imprecise, as expected. They indicate that the furnace cooled significantly more slowly during the flight than in pre-flight tests. Presumably, this is because of the absence of convection as a mechanism to remove heat.

The recorded temperatures are not precise enough to confirm that the desired supercooling interval, $\Delta T = 10°K$, was achieved. The reliability of temperature control proven during the pre-flight tests is the only evidence available to show that it was. More reliable control of ΔT could be achieved if the slider were modified to accommodate both the source and substrate crystals simultaneously as in Figure 1, so the saturation and growth steps could be performed without cooling to ambient temperature and reloading the slider. This would eliminate variations (e.g., small changes in voltages, resistances, and thermocouple positions) which may result from reloading the slider and making electrical interconnections with the rest of the payload, and which can affect temperature control and measurement. The desirability of this modification was recognized early in the program but could not be implemented because of scheduling constraints. The change

should be made before the experiment is performed again on a future SPAR or Space Transportation System flight. Better control of ΔT may be an important key to producing smoother films.

When the wafers were removed from the slider, one was found to have some cracks (Figure 13f). With subsequent handling, it broke into five fragments, but each was suitable for analysis, and the breakage did not cause any serious problem. The reason for the cracks is unknown.

The returned flight samples and several films grown during the pre-flight tests have been examined by conventional analytical techniques for characterizing semiconductor materials. The thickness, structural perfection, compositional homogeneity, and electrical properties have been evaluated and are discussed in this section.

A. Film Thickness

The thickness of the epitaxial films was determined by cleaving a narrow sliver from each wafer, etching it with a solution known as an "A-B etch", which makes the interface between the film and the substrate visible, and making a photomicrograph of the cross-section of the cleaved wafer. The film thickness is measured on the photomicrograph and divided by the magnification factor. The results are shown in Figure 14. Only one flight sample is shown because of the difficulty in obtaining a suitable cleavage of the other. The thickness of the films grown during the sounding rocket flight, 1.5 microns, is very nearly that predicted (see Equation 4, Section I). The films grown in normal gravity are about twice as thick, a result that was expected because of the contribution of natural convection to transport of the arsenic in the solutions. Although natural convection

does not have a serious effect on the quality of the films of the order of three microns thick, it is known to cause non-uniformity of thickness and surface roughness in thicker films[4].

B. X-ray Diffraction Topography

X-ray diffraction topographs of four pre-flight samples and of the flight samples are shown in Figure 15. They were recorded by the Berg-Barrett reflection technique with CuKα radiation and the 422 diffraction maximum.

The topographs of the pre-flight samples were recorded after Hall effect measurements (see below) were completed and after the slivers had been removed for thickness measurements. The film coverage area is more easily visible in the topographs than in the photographs in Figure 13. The bright areas in these topographs are shadows cast by metallic indium contacts applied for the Hall effect measurements. These topographs show that the films are single crystals of fairly good quality and uniform composition. One topograph, Figure 15a shows some contrast near the center, probably caused by strain in the film or substrate.

Likewise, the topographs of the flight samples show that the films are single and of fairly good quality and uniform composition. The topographs in Figure 15f are for the two largest fragments of the broken wafer. The light areas in the topographs of both flight samples are shadows cast by high regions on the somewhat rough surfaces.

C. Electrical Measurements

The Hall coefficient and resistivity of the samples were measured by the Van der Pauw technique. This technique allows the use of rectangular samples. It requires that four metallic electrical contacts be formed on the sample. Measurements were made at 300°K and 77°K. The data, summarized in Table 1, are as expected for n-type films on semi-insulating substrates. The sign of the Hall coefficient indicates that the films are n-type. Knowledge of the Hall coefficient and resistivity allows calculation of the net carrier concentration and the mobility, which are given in Table 1. The carrier concentration is one or two orders of magnitude greater than desired, but this result is probably acceptable because of the early stage of development of the LPE processor. It may be related to impurities derived from the stainless steel components of the furnace or from the hydrogen supply. The hydrogen was not purified by diffusion through palladium as is the usual practice. Photoluminescence measurements made on several samples in an effort to identify the impurities have not succeeded so far. The photoluminescence peak at 8210Å, normally found for this kind of film, is much broader and more symmetrical than usual. No other peaks were found in the range 7800 to 8500Å.

Identification and removal of the sources of any impurities before the experiment is repeated is desirable. Replacement of some of the stainless steel furnace components by fused quartz components, and better purification of the hydrogen are reasonable approaches.

REFERENCES

1. J. J. Hsieh, J. Crystal Growth 27, 49 (1974).
2. C. D. Thurmond, J. Phys. Chem. Solids 26, 785 (1965).
3. D. L. Rode, J. Crystal Growth 20, 13 (1973).
4. S. I. Long, J. M. Ballantyne, and L. F. Eastman, J. Crystal Growth 26, 13 (1974).

FIGURE CAPTIONS

1. Schematic drawing of apparatus for conventional gallium arsenide liquid phase epitaxy.
2. LPE processor, photographed after flight.
3. LPE processor with door open, showing end of furnace in which slider cartridge is inserted (furnace opening is covered with tape).
4. LPE processor with door open, showing other internal components.
5. LPE processor viewed from aft end with microprocessor section removed.
6. LPE processor, same view as Figure 5, but with insulation blanket removed.
7. Slider cartridge.
8. Graphite slider parts.
9. Schematic drawing of gas systems.
10. Temperature-time profile of film growth step.
11. Flow-rate meter calibration data.
12. Hydrogen consumption data.
13. Epitaxial films grown in LPE processor: a-d, pre-flight test samples; e-f, flight samples.
14. Microphotographs of cross-sections of LPE films: a-b, pre-flight test samples; c, flight sample.
15. X-ray diffraction topographs: a-d, pre-flight test samples; e-f, flight samples.

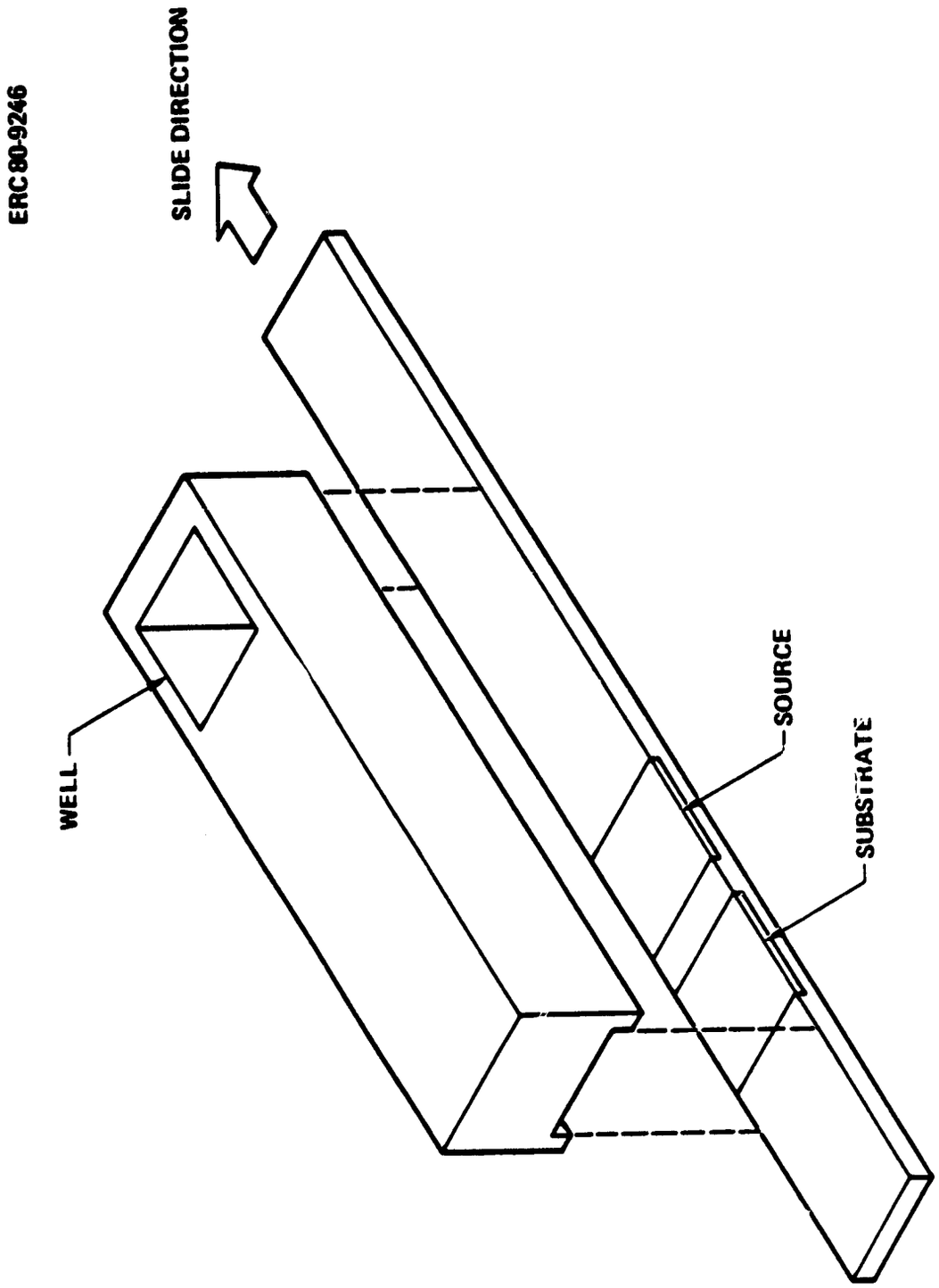

Fig. 1

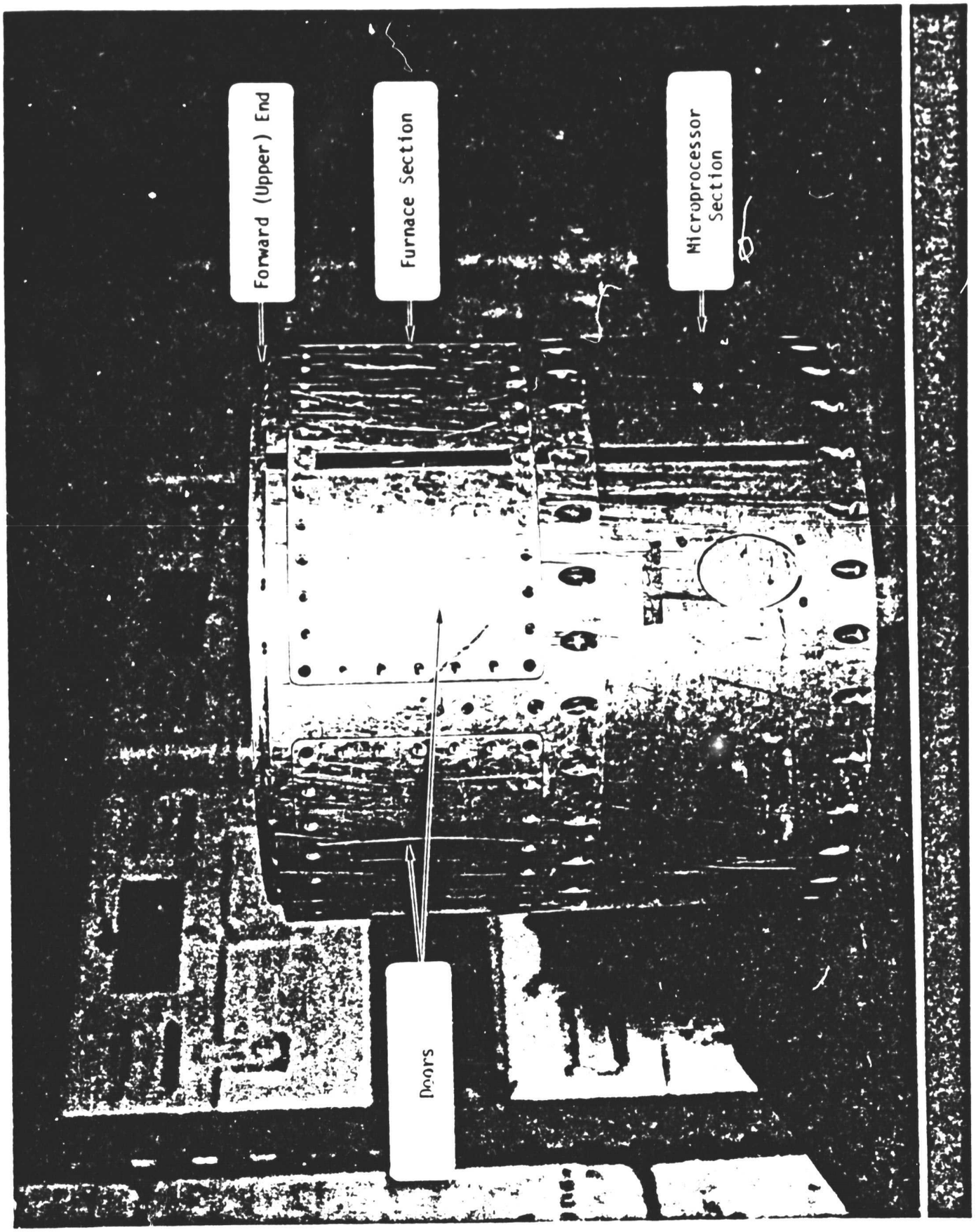
Forward (Upper) End
Furnace Section
Microprocessor Section
Doors

Fig. 2

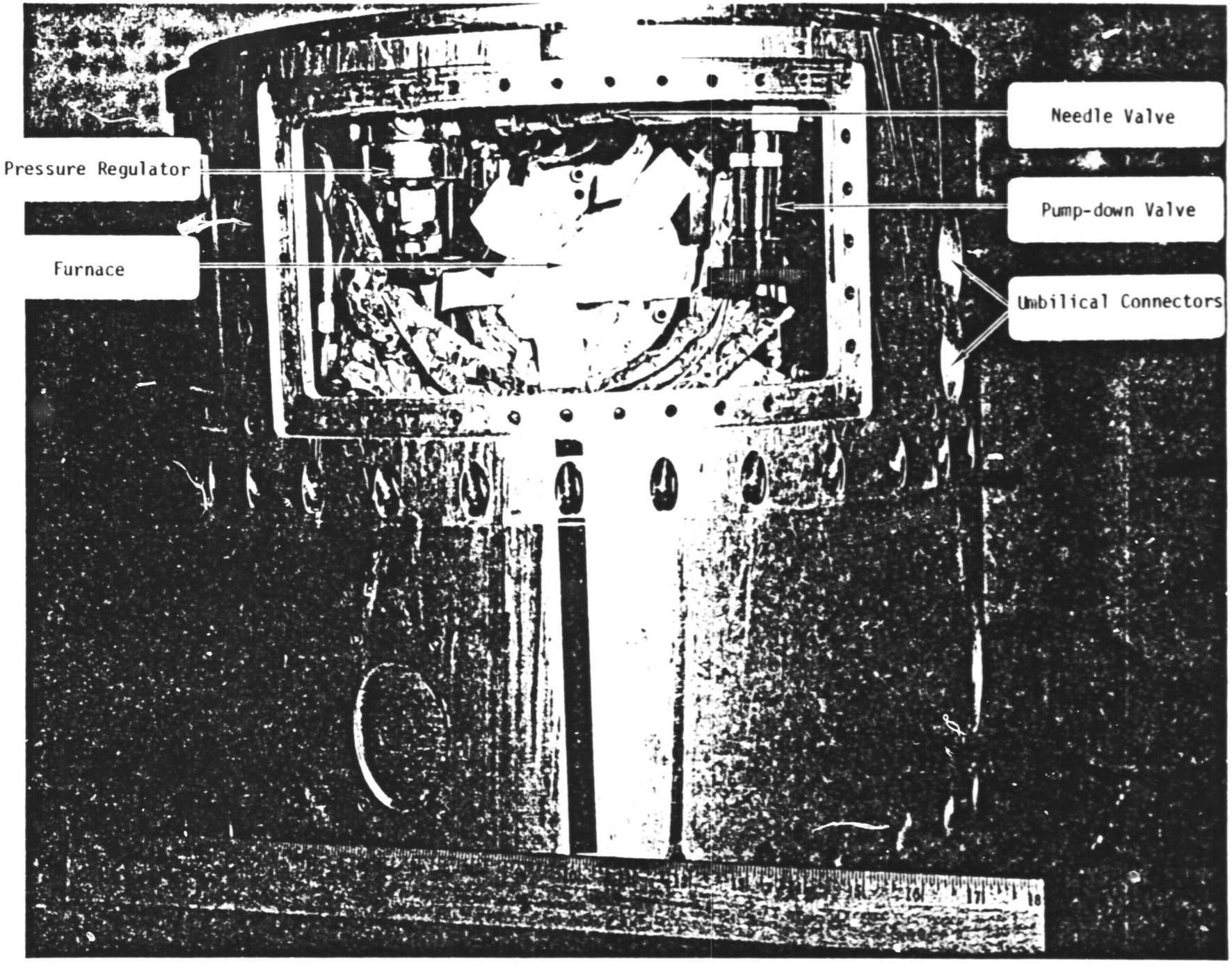
Needle Valve
Pressure Regulator
Pump-down Valve
Furnace
Umbilical Connectors

Fig. 3

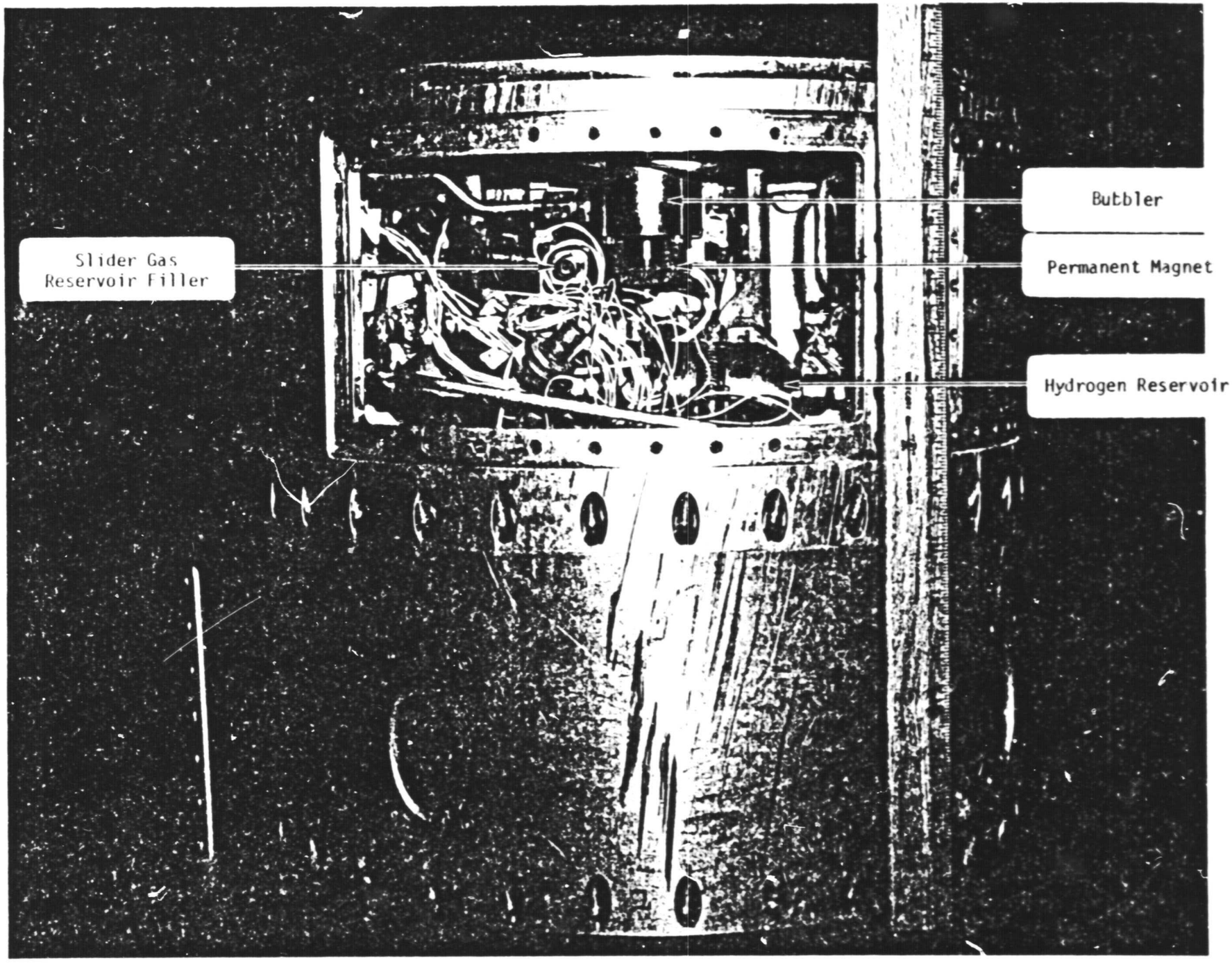
Slider Gas
Reservoir Filler
Bubbler
Permanent Magnet
Hydrogen Reservoir

Fig. 4

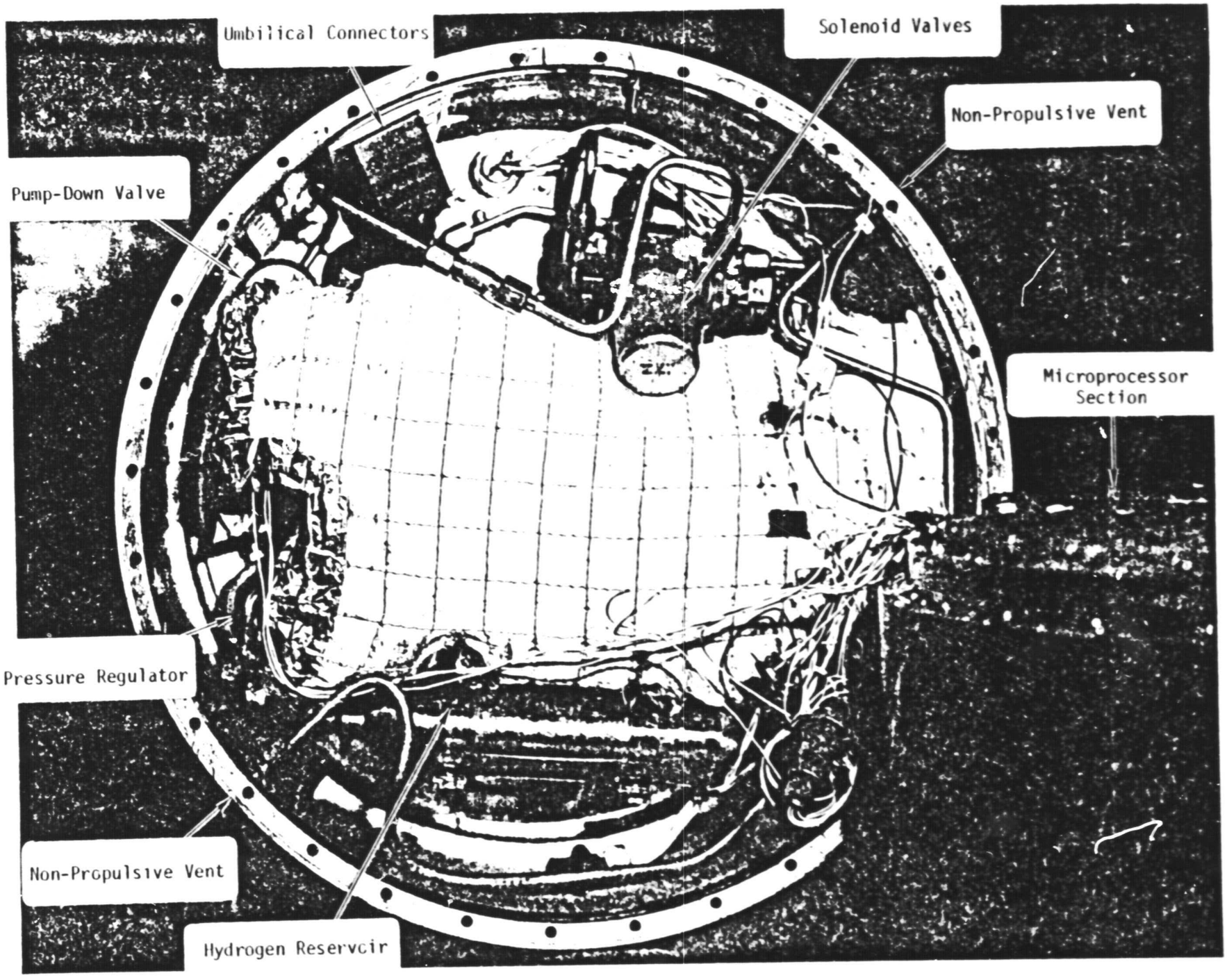
Umbilical Connectors
Solenoid Valves
Non-Propulsive Vent
Pump-Down Valve
Microprocessor Section
Pressure Regulator
Non-Propulsive Vent
Hydrogen Reservoir

Fig. 5

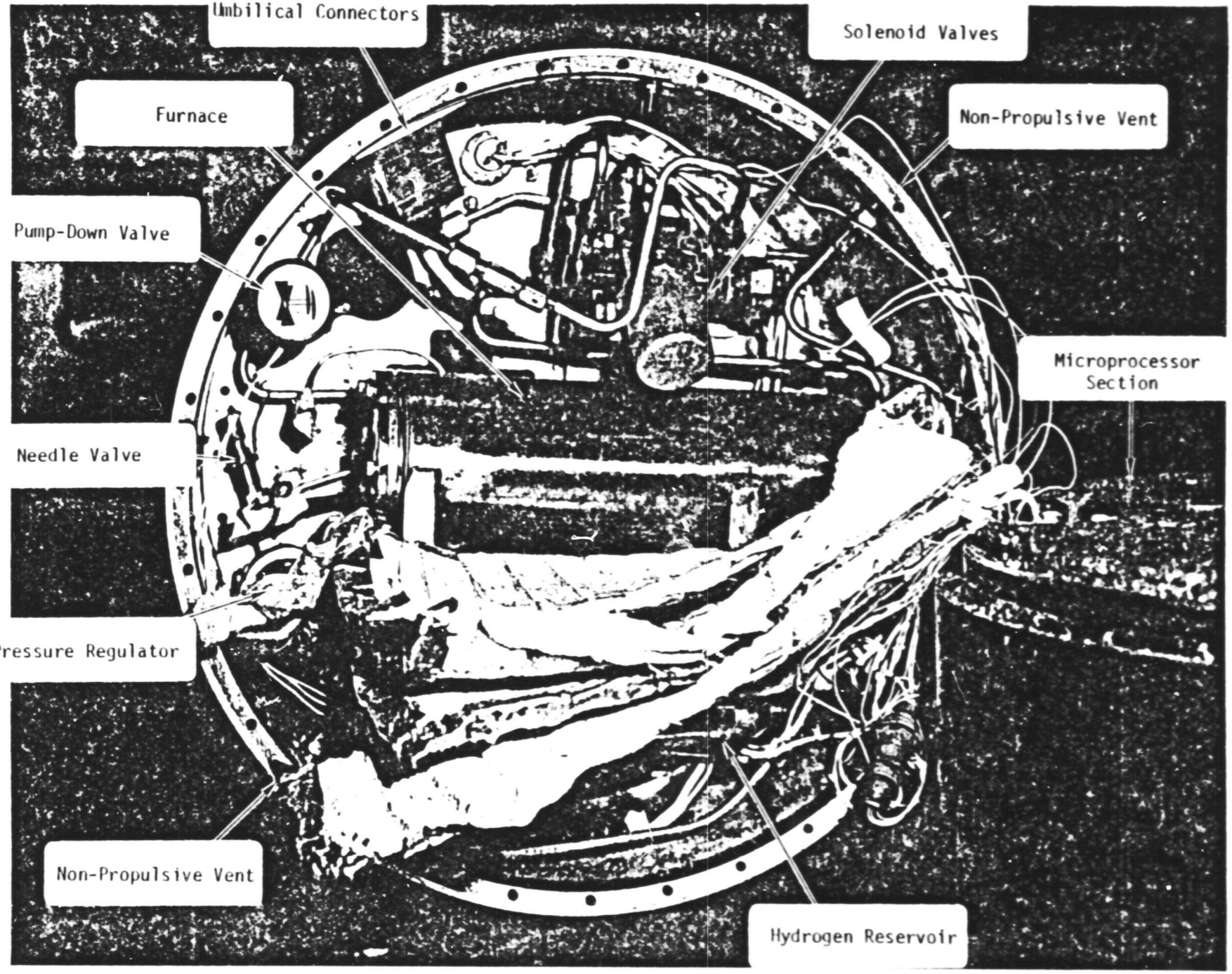
Umbilical Connectors
Solenoid Valves
Furnace
Non-Propulsive Vent
Pump-Down Valve
Microprocessor Section
Needle Valve
Pressure Regulator
Non-Propulsive Vent
Hydrogen Reservoir

Fig. 6

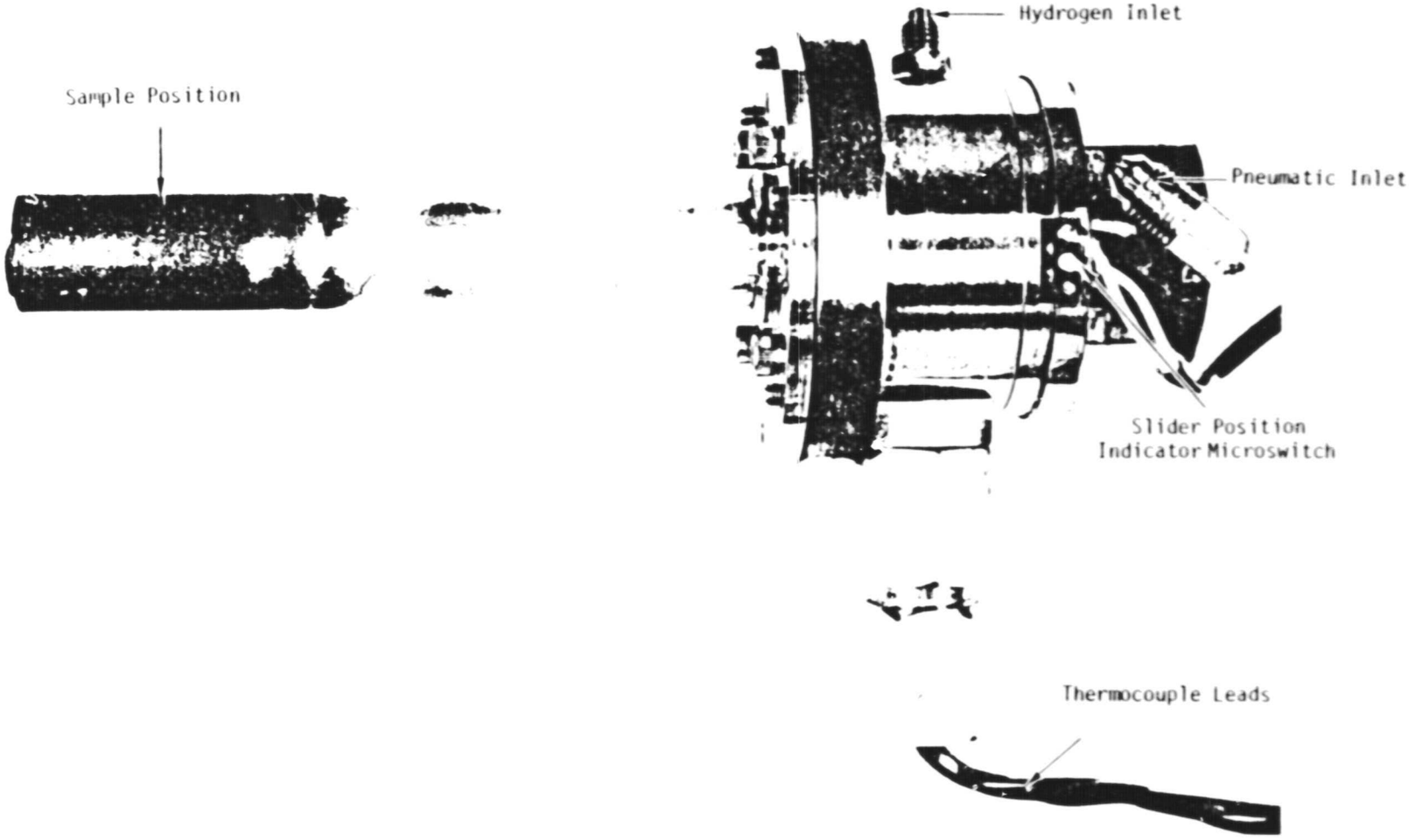

Fig. 7

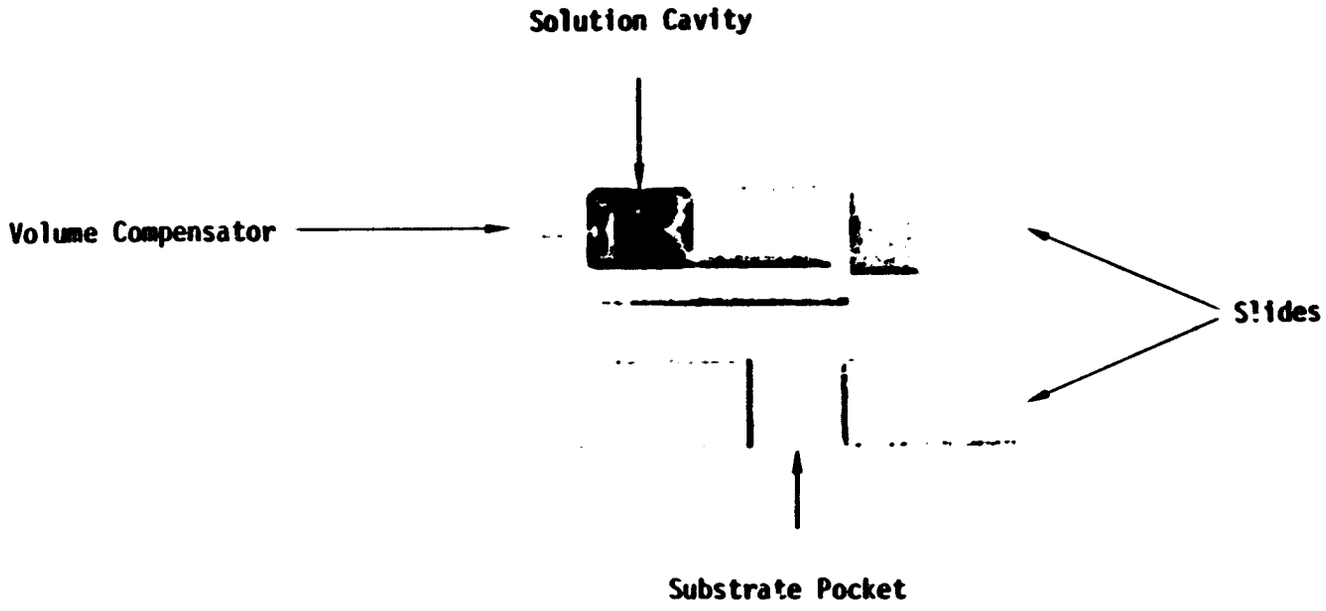

Fig. 8

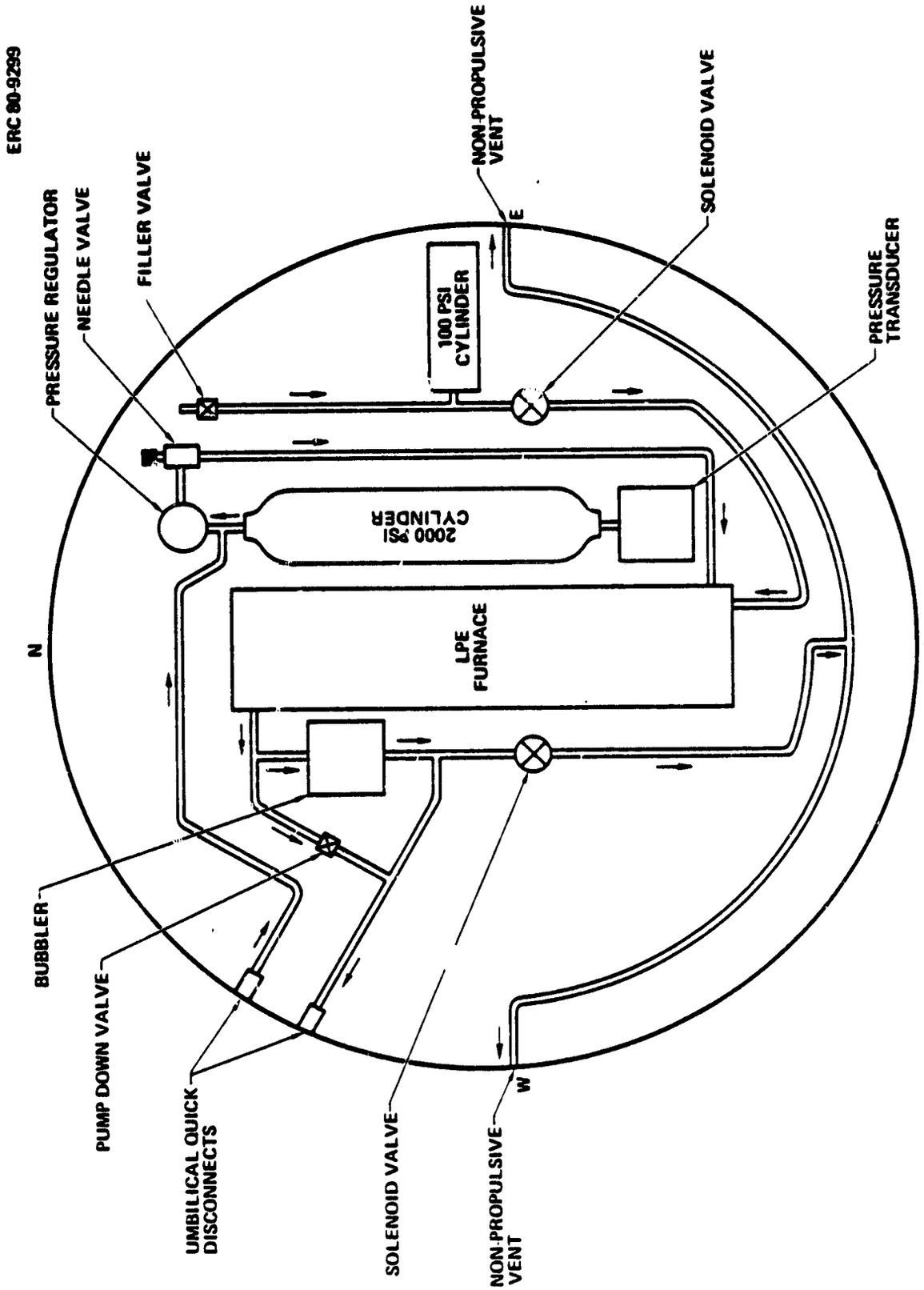
ERC 80-9299
PRESSURE REGULATOR
NEEDLE VALVE
FILLER VALVE
NON-PROPULSIVE VENT
SOLENOID VALVE
PRESSURE TRANSDUCER
100 PSI CYLINDER
2000 PSI CYLINDER
LPE FURNACE
N
E
S
W
BUBBLER
PUMP DOWN VALVE
UMBILICAL QUICK DISCONNECTS
SOLENOID VALVE
NON-PROPULSIVE VENT

Fig. 9

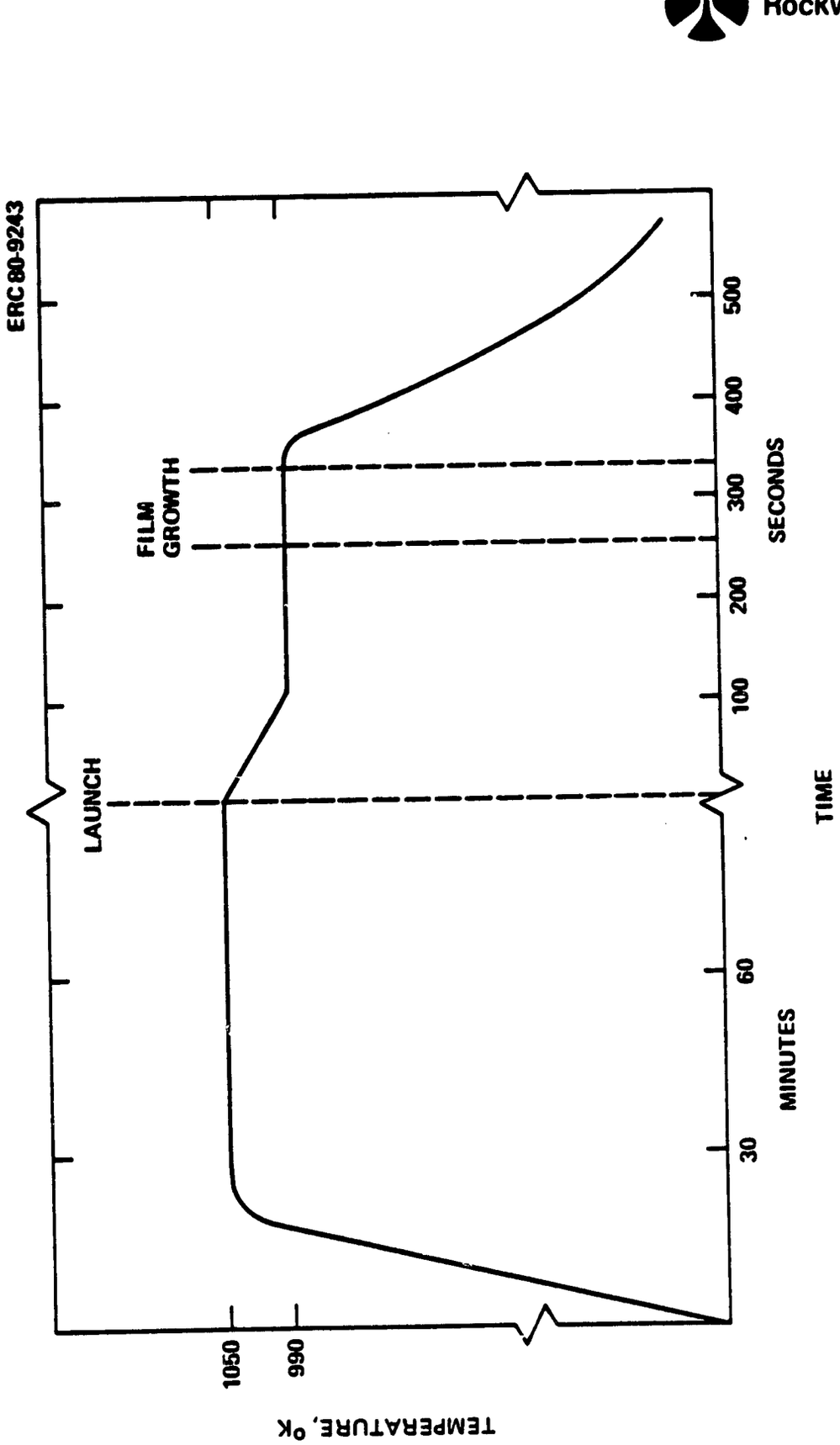
ERC 80-9243
FILM GROWTH
LAUNCH
TEMPERATURE, °K
1050
990
MINUTES
30
60
TIME
SECONDS
100
200
300
400
500

Fig. 10

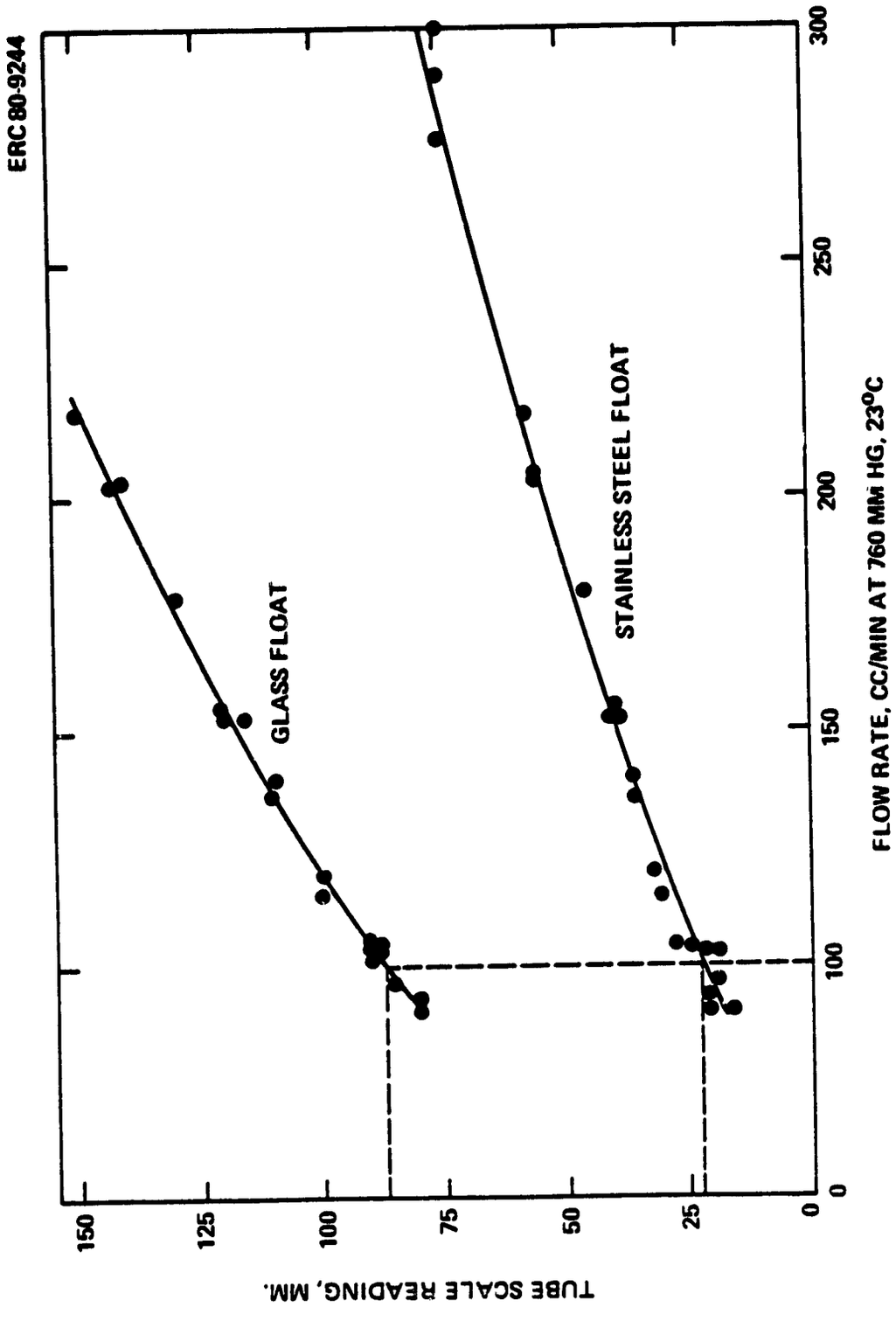
ERC 80-9244
GLASS FLOAT
STAINLESS STEEL FLOAT
TUBE SCALE READING, MM.
FLOW RATE, CC/MIN AT 760 MM HG, 23°C
0
25
50
75
100
125
150
0
100
150
200
250
300

Fig. 11

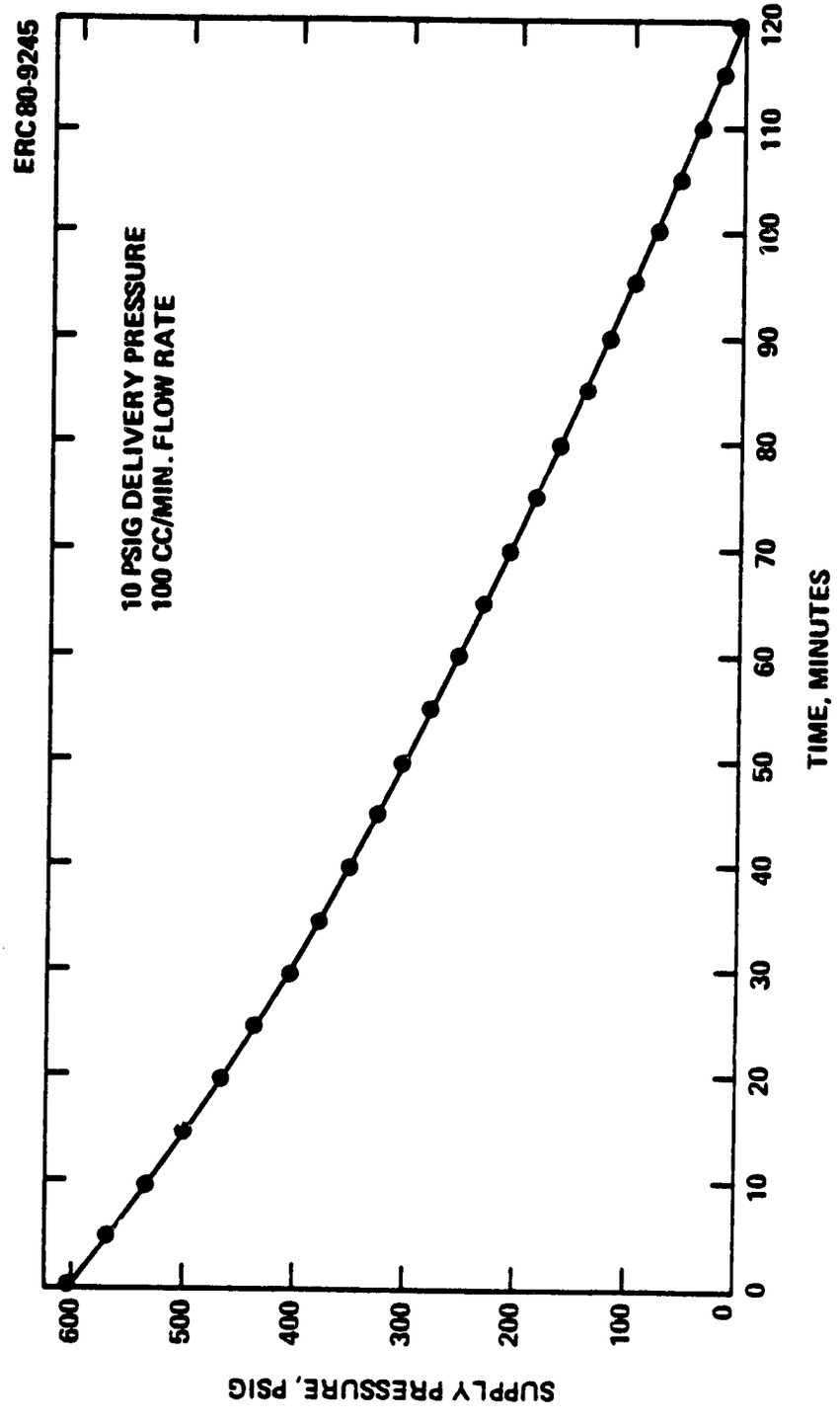
ERC80-9245
10 PSIG DELIVERY PRESSURE
100 CC/MIN. FLOW RATE
SUPPLY PRESSURE, PSIG
600
500
400
300
200
100
0
TIME, MINUTES
0
10
20
30
40
50
60
70
80
90
100
110
120

Fig. 12

(b)

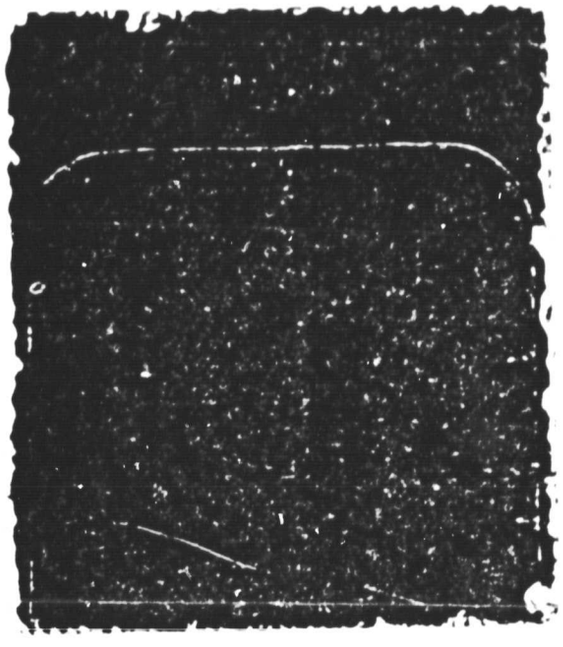

(d)

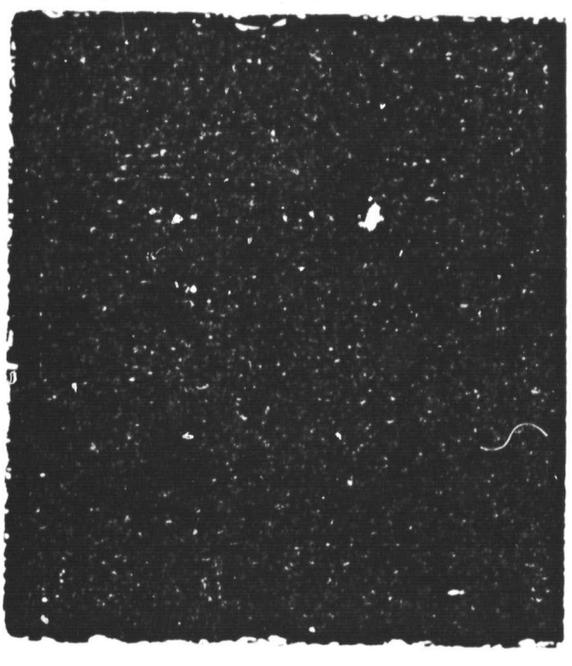

(a)

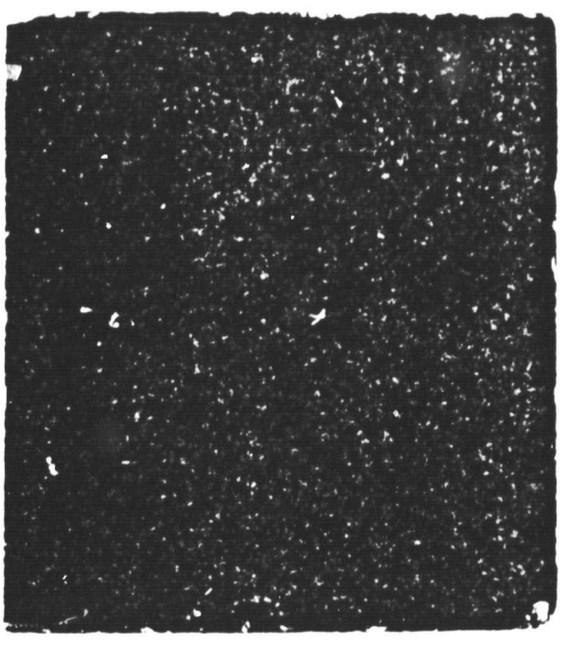

(c)

Fig. 13

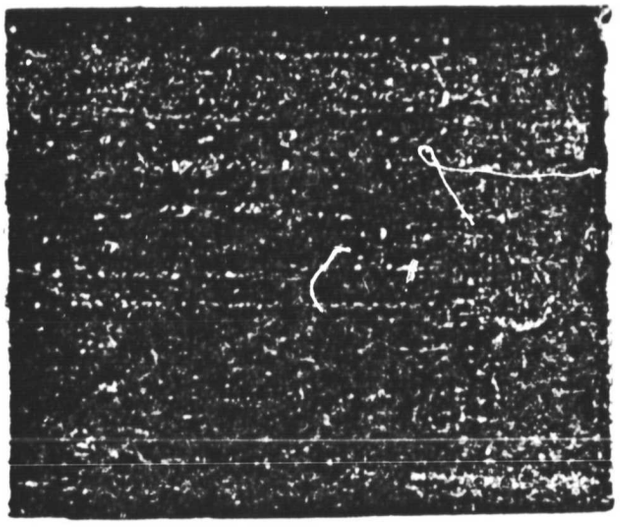

(e)

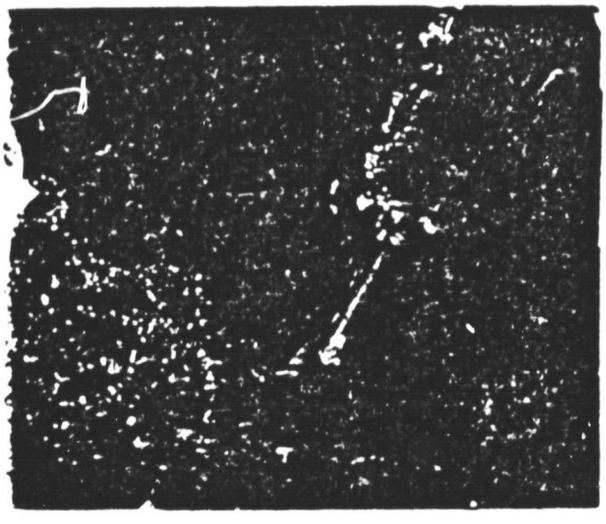

(f)

Fig. 13 (Cont'd.)

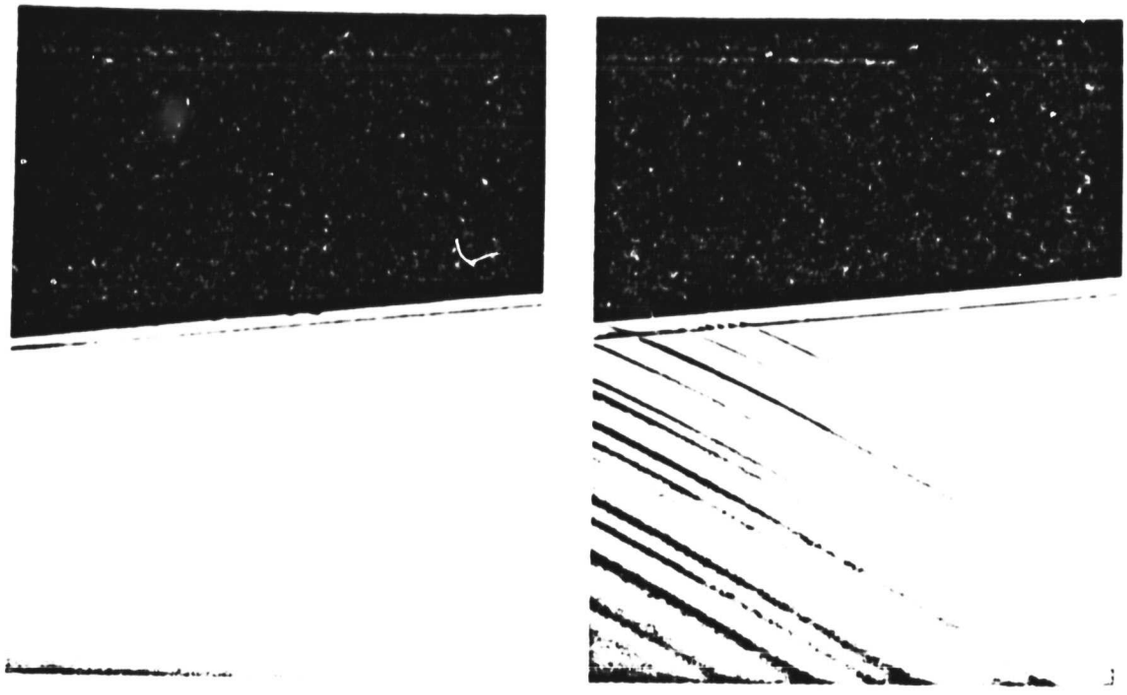

(a)

(b)

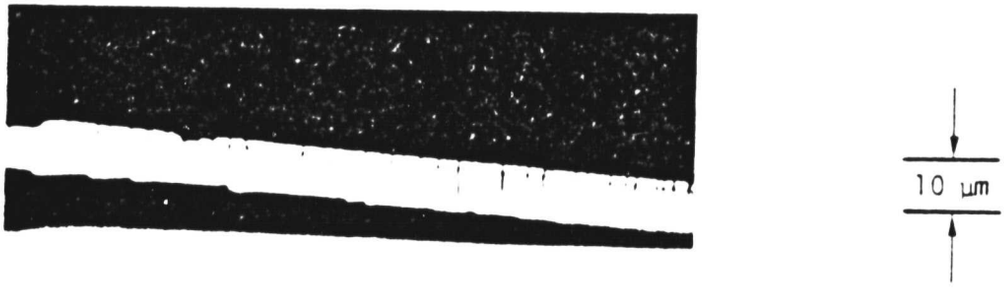

(c)

Fig. 14

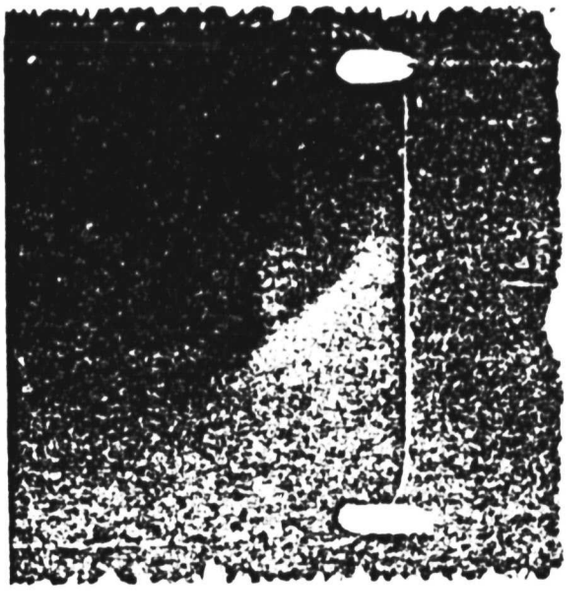

(a)

(b)

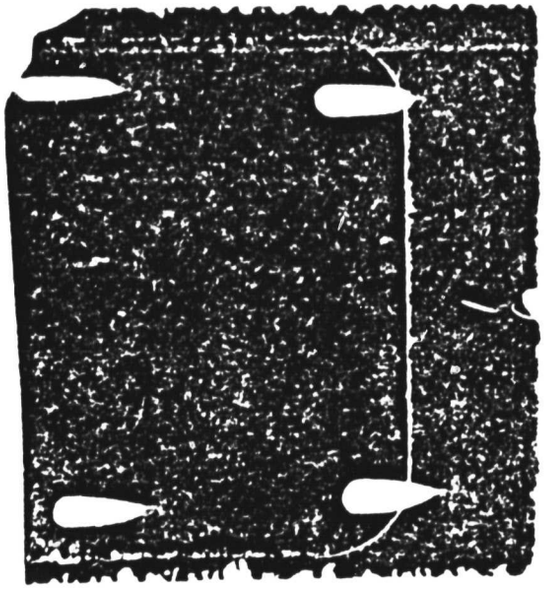

(c)

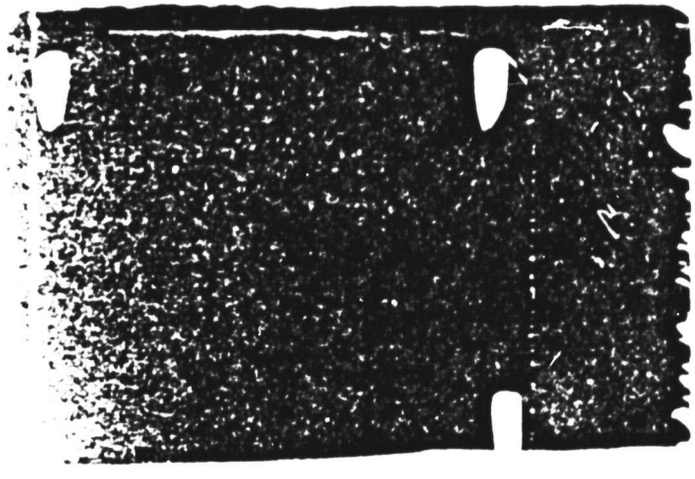

(d)

Fig. 15

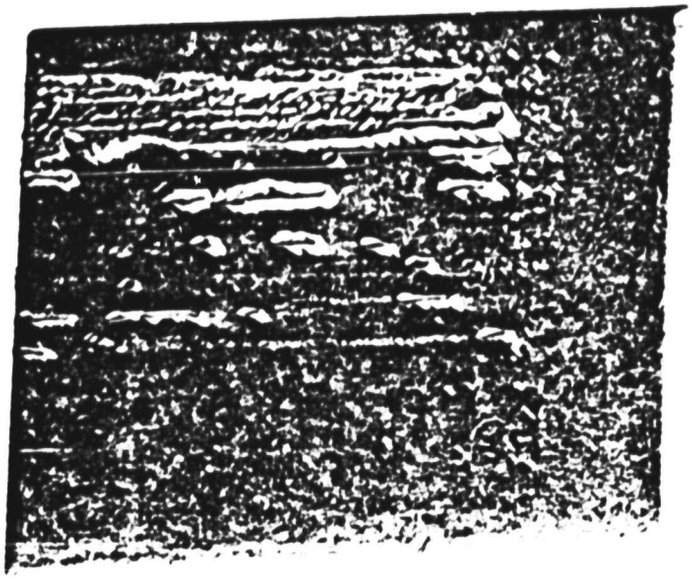

(e)

(f)

Fig. 15, Cont'd.